Dynamics of Cooper Pair Formation in $Bi_2Sr_2CaCu_2O_{8+\delta}$

Robert A. Kaindl, Marc A. Carnahan, and Daniel S. Chemla
Department of Physics, University of California at Berkeley, and Materials Sciences Division, E. O. Lawrence Berkeley National Laboratory, Berkeley, CA 94720

Seongshik Oh* and James N. Eckstein
Department of Physics, University of Illinois, Urbana, IL 61801

We report the first ultrafast measurements of the transient terahertz conductivity in the high-T_C superconductor $Bi_2Sr_2CaCu_2O_{8+\delta}$. After depletion of the superconducting condensate by optical excitation, the ensuing dynamics is tracked with high sensitivity at various excitation densities and temperatures. We measure low-energy spectra and shapes of decay that demonstrate a bimolecular kinetics of condensate formation on a picosecond timescale and yield a measure of quasiparticle interactions hidden in linear spectroscopy.

PACS numbers: 78.47.+p, 74.72.Hs, 74.40.+k, 74.25.Gz

In high-T_C cuprate superconductors, the nature of the charge carriers and the microscopic interactions that mediate their pairing at transition temperatures of $T_C \approx 100$ K are still unresolved[1,2]. A key microscopic process in a superconductor concerns the interaction between two quasiparticles as they form a Cooper pair. A fine balance exists in thermal equilibrium, in which the rates of Cooper pair formation and breakup are matched. However, the interactions may be directly revealed by following the dynamics of a nonequilibrium density of excess quasiparticles in time. A potentially powerful tool to study these phenomena is ultrafast time-resolved spectroscopy, which was successfully used to probe fundamental carrier interactions in semiconductors or molecular structural dynamics resonant to their transitions[3,4].

This has inspired time domain experiments on high–T_C cuprates, almost all of them probing the optical reflectivity at energies $E \approx 1.5$ eV[5–12]. Recently, intensity-dependent decay rates gave evidence for biparticle interactions, but contradicting explanations were offered involving either recombination or thermalization of quasiparticles[8,9]. This uncertainty arises because visible probes detect reflectivity changes energetically far above the intrinsic low-energy excitations of a superconductor. In contrast, the low-energy electromagnetic response at terahertz (THz) frequencies couples directly to quasiparticles and Cooper pairs. It can be expressed by the frequency-dependent complex conductivity $\sigma(\omega) = \sigma_1(\omega) + i\sigma_2(\omega)$ governing the currents induced by a transverse THz electromagnetic field[13]. A first ultrafast study with THz pulses indicated picosecond condensate recovery in $YBa_2Cu_3O_{7-\delta}$, although a microscopic process underlying the kinetics was not discerned[12].

In this paper we report experiments that detect ultrafast changes in the THz conductivity of $Bi_2Sr_2CaCu_2O_{8+\delta}$ (Bi-2212) for the first time. We identify a partial depletion of the superconducting condensate after optical excitation and track its temporal kinetics on a picosecond timescale. The transient THz spectra demonstrate a bimolecular kinetics of condensate formation at low temperatures and a thermally-induced crossover in shape, providing direct evidence for pairwise recombination of quasiparticles into Cooper pairs.

We investigate near optimally-doped Bi-2212 with a superconducting transition temperature $T_C \approx 88$ K. Highly crystalline, c-axis oriented films of 62-nm thickness were grown on $LaAlO_3$ substrates by atomic layer-by-layer molecular beam epitaxy[14]. The superconductor is excited with ultrashort near-infrared (1.55 eV) pump pulses from a high repetition-rate Ti:sapphire amplifier system. Picosecond THz probe pulses covering the range of ≈3–12 meV photon energy are generated and detected via optical rectification and electro-optic sampling in ZnTe[15]. For each pump-probe delay, we record the THz electric field waveforms transmitted through the sample in equilibrium and in the transient excited state, respectively. Fourier transformation of the fields and straightforward electrodynamical relations[16] yield both the equilibrium value of the frequency-dependent CuO_2-plane THz conductivity $\sigma(\omega)$ and its pump induced transient change $\Delta\sigma(\omega)$. Real and imaginary parts of conductivity are obtained on equal footing, and their concurrent availability is essential for understanding the transient state.

The equilibrium THz conductivity is displayed in Fig. 1. We observe significant changes as the temperature is reduced from the normal state at $T = 95$ K (triangles) to $T = 6$ K (circles) well below T_C. The conductivity within this spectral range can be described by the well-known two-fluid model

$$\sigma(\omega) = \rho_{QP} \frac{1}{1/\tau - i\omega} + \rho_S \left\{ \pi\,\delta(\omega) + \frac{i}{\omega} \right\} \quad (1)$$

where ρ_{QP} and ρ_S denote the quasiparticle and superfluid densities[2]. The first term is a Drude response of quasiparticles with momentum scattering rate $1/\tau$. This component (thin lines) fully accounts for the broadband conductivity above T_C. The ρ_S term in Eq. 1 constitutes the superfluid response emerging below T_C. Its temperature dependence as obtained from fits to the data is

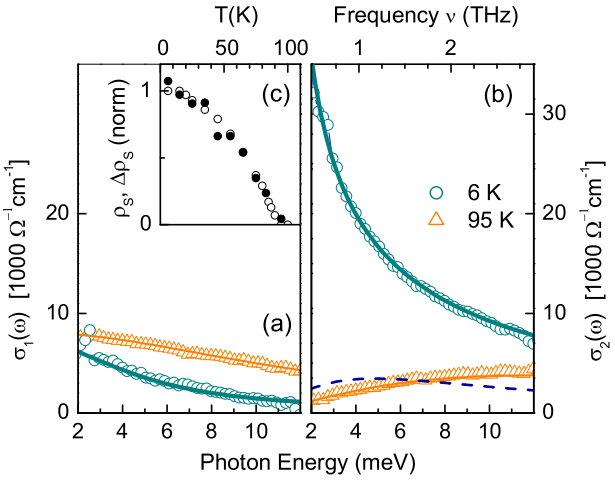

FIG. 1: (color online). Equilibrium THz conductivity of Bi-2212, showing (a) real part $\sigma_1(\omega)$ and (b) imaginary part $\sigma_2(\omega)$ of conductivity at the temperatures indicated. Solid lines are fits using a two-fluid model (see text). In the normal state ($T = 95$ K) this yields a spectral weight $(\hbar^2/\epsilon_0)\rho_{QP} = 0.75$ eV^2 and a Drude scattering rate $1/\tau = 3$ THz similar to previous work[28]. At $T = 6$ K, the condensate spectral weight is $(\hbar^2/\epsilon_0)\rho_S = 0.5$ eV^2. A residual quasiparticle weight of $\rho_{QP}(6K)/\rho_{QP}(95K) \approx 34\%$ remains with a reduced scattering rate $\tau^{-1} = 1.20$ THz. Dashed line: imaginary part corresponding to the residual 6 K quasiparticle spectral weight. (c) Temperature dependence of superfluid density ρ_S (open circles) and initial photoinduced spectral weight change $\Delta\rho_S$ (solid dots) obtained from two-fluid fits to equilibrium and transient THz spectra, respectively.

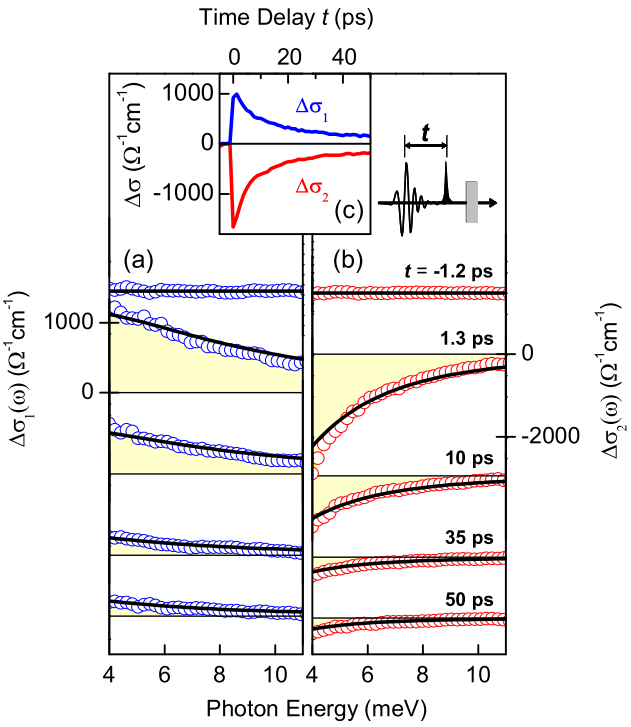

FIG. 2: (color online). Induced THz conductivity changes, for $T = 6$ K and $I_0 \equiv 0.7$ μJ/cm^2 excitation fluence. (a),(b) Measured changes in the real part of conductivity $\Delta\sigma_1$ and the imaginary part $\Delta\sigma_2$ (circles) at indicated time delays t after excitation. Solid lines: two-fluid model, corresponding to momentary depletion of 16% (1.3 ps), 8% (10 ps), 3.2% (35 ps), and 2.7% (50 ps) of the low-temperature condensate spectral weight and Drude widths, respectively, of $1/\tau = 1.35, 1.26, 1.21$ and 1.20 THz. (c) Transient conductivity changes at center probe energy 5.5 meV (averaged over 1.6 meV interval) versus pump-probe time delay.

shown in Fig. 1c (open circles). Notably, the δ-function describing the infinite d.c. conductivity (Eq. 1) is accompanied by a characteristic inductive response of dissipationless supercurrents scaling as $1/\omega$ in σ_2. It is largest at low frequencies, where σ_2 predominantly samples the superfluid density. Conversely, the real part σ_1 is reduced at $T = 6$ K (circles, Fig. 1a), although a significant fraction remains due to nanoscale electronic inhomogeneities in this superconductor[17]. Within our model, the missing quasiparticles are condensed into the superfluid, $\rho_S(6K) = \rho_{QP}(95K) - \rho_{QP}(6K)$, and the expected low-temperature imaginary part σ_2 (thick line, Fig 1b) agrees well with experiment. While a fraction stems from the residual quasiparticles (dashed line), $\sigma_2(\omega)$ is dominated by the $1/\omega$ response of the condensate.

Nonequilibrium changes $\Delta\sigma(\omega)$ of the THz conductivity in the superconducting state are shown in Fig. 2 (circles) for different time delays t after optical excitation. Immediately after excitation ($t = 1.3$ ps), the spectra exhibit a strongly frequency-dependent reduction $\Delta\sigma_2 < 0$ of the imaginary part, along with a marked increase of the real part $\Delta\sigma_1 > 0$. Signs and shapes of these features indicate a reduced density of the superconducting condensate, with the spectral weight transferred into quasiparticle excitations. This is confirmed by corresponding changes predicted by the two-fluid model (solid lines), with conserved spectral weight $\Delta\rho_S = -\Delta\rho_{QP}$ and a small increase of $1/\tau$, which closely follow the experimental observations[18]. At this fluence, the initial spectral weight transfer to finite frequencies in σ_1 corresponds to a 16% reduction of the superconducting condensate, or $(\hbar^2/\epsilon_0)\Delta\rho_S \approx -0.08$ eV^2. The breakup of Cooper pairs into quasiparticles arises on a sub-picosecond timescale via interactions with the initially photoexcited carriers. At longer time delays, the conductivity spectra and the time dependence of the transient conductivity (Fig. 2c) show the concurrent decay of condensate depletion and excess quasiparticles on a 10 ps timescale. This relaxation, therefore, does not represent mere intraband thermalization of quasiparticles but arises from their conversion back into Cooper pairs.

The photoinduced initial spectral weight transfer subsides with rising temperature (Fig. 1c, solid dots) and closely follows the superfluid condensate obtained from the equilibrium spectra, $\Delta\rho_S \propto \rho_S$. If each absorbed photon (energy $\hbar\omega_P$) were fully dissipated into broken Cooper pairs of energy 2Δ, the density of generated qua-

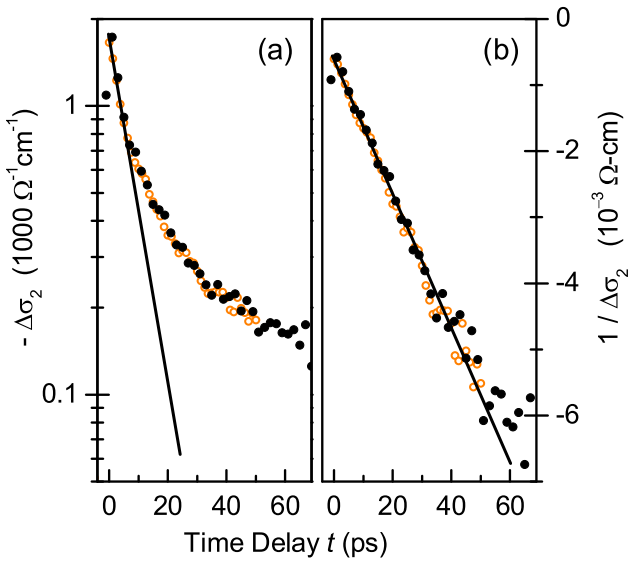

FIG. 3: (color online). Bimolecular temporal kinetics of condensate recovery at $T = 6$ K. The identical transient conductivity $\Delta\sigma_2(t)$ is plotted (a) on a logarithmic scale and (b) as the reciprocal $1/\Delta\sigma_2$. Data are averaged over a 1.6 meV interval at center probe energy 5.5 meV, for excitation fluence $I = I_0$. Equivalent dynamics is observed in the real part $\Delta\sigma_1$ (not shown). Solid lines are guides to eye, open and closed circles denote scans taken on different days.

siparticle excitations would scale as $\propto \hbar\omega_P/2\Delta$. Then, $\Delta\rho_S$ should rise with increasing temperature T as 2Δ falls, in striking contrast to the observation. Instead, Fig 1c demonstrates that a constant *fraction* of Cooper pairs is initially broken at each temperature T. We can understand this as a competition between Cooper pair breakup and phonon emission, as the photoexcited carriers scatter multiple times before losing their initial 1.5 eV energy. The occupation density of high-energy phonons is small, and accordingly their emission rate remains largely constant for $T < 100$ K. Inelastic scattering with Cooper pairs, in contrast, will follow a rate proportional to the density ρ_S (each Cooper pair exhibiting a constant cross section for breakup). The different probabilities of these relaxation channels can thus explain the observed temperature dependence.

A central aspect of our study concerns the temporal shape of decay. The recovery dynamics at $T = 6$ K is strongly non-exponential as evident from Fig. 3a, where $\Delta\sigma_2$ is shown on a logarithmic scale. However, a strikingly simple description of the observed kinetics is obtained by plotting the *reciprocal* $1/\Delta\sigma_2$ in Fig. 3b, which reveals a linear time dependence

$$\frac{1}{\Delta\sigma_2(t)} = \frac{1}{\Delta\sigma_2(0)} + r\,t$$

with slope r. Differentiation in time yields $d/dt\ \Delta\sigma_2 = -r\,(\Delta\sigma_2)^2$. This is the well-known hallmark of *bimolecular* kinetics, analogous to binary chemical reactions or hole capture dynamics in semiconductors[19]. With transient conductivity changes proportional to the departure of condensate and quasiparticles from equilibrium $\Delta\rho \propto \Delta\sigma$, the natural explanation of this kinetics is therefore a pairwise interaction of excess carriers that annihilate as they recombine into Cooper pairs. Scaling the changes in Fig. 3b in terms of spectral weight yields $r = 2$ eV^{-2}ps^{-1}. An analysis of the two-fluid fits to the transient spectra confirms that $\Delta\rho_S$ exhibits the same kinetics as $\Delta\sigma_2$, corroborating this picture of bimolecular condensate recovery. The scenario is further substantiated by the density dependence at low temperatures, Fig. 4a, which shows the persistence of a bimolecular decay shape at different excitation densities.

Quasiparticle interactions in superconductors have been theoretically described by kinetic equations[20,21], thermodynamic models[22], or the Rothwarf-Taylor rate equation[23,24]

$$\frac{d}{dt}n^* = -R\,(n^*)^2 - 2R\,n_T\,n^* + 2\tau_B^{-1}N_\omega^*, \qquad (2)$$

where n^* is the excess (photoexcited) quasiparticle density, n_T the equilibrium (thermally excited) quasiparticle density, and R the effective recombination coefficient. Quasiparticle loss occurs via mutual recombination of two excess quasiparticles, as described by the $(n^*)^2$ term, or via interaction of a single excess quasiparticle with an equilibrium one ($n_T n^*$-term). The reverse process of Cooper-pair breakup through absorption of a non-equilibrium boson (density N_ω^*) is described by the third term and leads to quasiparticle generation at rate $2\tau_B^{-1}$. In conventional superconductors, "phonon trapping" occurs where acoustic phonons emitted during recombination lack efficient decay channels and thus regenerate quasiparticles through Cooper-pair breakup. This masks the pairwise nature of the kinetics, which becomes dominated by the slow (typically nanosecond) single-exponential decay of acoustic phonons observed in time-resolved experiments[25]. The bimolecular decays of the THz conductivity in Bi-2212, in contrast, demonstrate the absence of boson trapping and point towards a fast decay and inefficient reabsorption of the phonons or spin fluctuations emitted during Cooper pair formation. Quasiparticles at the anti-nodes of the d-wave gap in cuprates emit high-energy bosons ($2\Delta_0 \approx 60$ meV) whose lifetimes are short and whose resulting lower-energy decay products can experience increased kinematic restrictions for Cooper pair breakup[26]. At low temperatures and sufficiently high excitation densities ($n^* \gg n_T$), the quadratic term in Eq. 2 survives which explains the observed bimolecular kinetics.

At higher temperatures, the thermal quasiparticle density becomes large compared to the photoexcited quasiparticle density, or $n_T > n^*$. The second term in Eq. 2 then dominates, predicting a single-exponential relaxation. Experiments at elevated temperatures are shown in Fig. 4b (symbols). Indeed, with increasing temperature the shapes of decay evolve from purely bimolecular

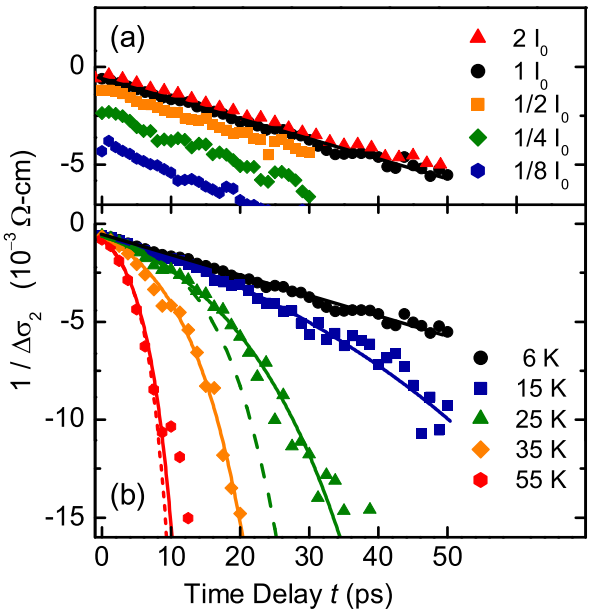

FIG. 4: (color online). Density and temperature dependence of conductivity dynamics, displayed as $1/\Delta\sigma_2(t)$ for 5.5 meV probe energy. (a) Decays for different excitation intensities I as indicated, at $T = 6$ K and with I_0 defined as in Fig 2. Solid line: guide to the eye indicating bimolecular decay. (b) Kinetics for different temperatures as indicated, at $I = I_0$. Solid lines are fits using the model described in the text, with constant bimolecular coefficient and $2Rn_T = 0, 0.02, 0.06, 0.12, 0.26$ THz (lowest to highest temperature). For comparison, single-exponential kinetics is shown as least square fits to the data over its entire range at 25 K (long-dashed line, decay time $\tau = 7.9$ ps) and 55 K (short-dashed line, $\tau = 3.1$ ps).

at $T = 6$ K to a kinetics at 55 K closely modeled by a $\tau \approx 3$ ps single-exponential decay (short-dashed line). Intermediate temperatures exhibit mixed dynamics, as illustrated by the lack of agreement with a purely single-exponential decay at $T = 25$ K (long-dashed line). The kinetics at all temperatures are well reproduced by solutions of Eq. 2 (solid lines, Fig. 4b) with varying thermally excited quasiparticle density n_T. Moreover, we note that only the thermally activated quasiparticles interact strongly to affect the kinetics, whereas the $T = 6$ K residual Drude spectral weight (Fig. 1) bears no influence on the low-temperature kinetics. Even at $T = 55$ K, the thermally activated Cooper pair formation contributes a lifetime broadening of only $\hbar/\tau = 0.2$ meV which remains far below the photohole linewidths in angle-resolved photoemission studies[27] or the broadening of THz spectra in Bi-2212(Fig. 1). This underscores the distinctly different physics: while elastic scattering with large momentum transfer dominates transport properties of carriers, the transient THz kinetics enables a sensitive measure of less frequent inelastic quasiparticle recombination.

Photoexcitation of the high-T_C cuprate superconductor Bi-2212 thus leads to an ultrafast depletion of the superconducting condensate and concomitant rise of quasiparticle absorption. The ensuing transient THz conductivity spectra and their time, temperature, and density dependence provide strong evidence for a quasiparticle-quasiparticle scattering process that underlies pairwise recombination into Cooper pairs.

We thank M. Woerner, J. Orenstein, and D.-H. Lee for helpful discussions. This work was supported by the Director, Office of Science, Basic Energy Sciences, U.S. Department of Energy, under contract DE-AC02-05CH11231 and the Fredrick Seitz Materials Research Lab at UIUC. R.A.K. gratefully acknowledges support through the Deutsche Forschungsgemeinschaft.

* Present address: National Institute of Standards and Technology, Boulder, CO 80305

[1] M. R. Norman and C. Pépin, Rep. Prog. Phys. **66**, 1547 (2003).
[2] J. R. Waldram, *Superconductivity of Metals and Cuprates*, Institute of Physics Publishing, Bristol and Philadelphia (1996).
[3] J. Shah, *Ultrafast Spectroscopy of Semiconductors and Semiconductor Nanostructures*, Springer Verlag, (1999).
[4] A. Douhal and J. Santamaria (Eds), *Femtochemistry and Femtobiology*, World Scientific, Signapore (2002).
[5] C. J. Stevens *et al.*, Phys. Rev. Lett. **78**, 2212 (1997).
[6] S. G. Han, Z. V. Vardeny, K. S. Wong, O. G. Symko, and G. Koren, Phys. Rev. Lett. **65**, 2708 (1990).
[7] V. V. Kabanov, J. Demsar, B. Podobnik, D. Mihailovic, Phys. Rev. **B59**, 1497 (1999).
[8] P. Gay *et al.*, J. Low Temp. Physics **117**, 1025 (1999).
[9] G. P. Segre *et al.*, Phys. Rev. Lett. 88, 137001 (2002); N. Gedik *et al.*, Phys. Rev. B**70**, 014504 (2004).
[10] M. L. Schneider *et al.*, Eur. Phys. J. B**36**, 327 (2003).
[11] R. A. Kaindl *et al.*, Science **287**, 470 (2000).
[12] R. D. Averitt *et al.*, Phys. Rev. **B63**, 140502 (2001).
[13] M. Dressel and G. Grüner, *Electrodynamics in Solids*, p. 61, Cambridge University Press (2002).
[14] J. N. Eckstein and I. Bozovic, Ann. Rev. Mat. Sci. **25**, 679 (1995).
[15] Z. G. Lu, P. Campbell, and X.-C. Zhang, Appl. Phys. Lett. **71**, 593 (1997).
[16] see e.g. R. A. Kaindl *et al.*, Phys. Rev. Lett. **88**, 027003 (2002) and references therein.
[17] J. E. Hoffman *et al.*, Science **297**, 1148 (2002); J. Corson *et al.* Phys. Rev. Lett. **85**, 2569 (2000). A partial condensate spectral weight transfer to GHz frequencies occurs but leaves the response above ≈ 1 THz unaffected.
[18] Note that the small increase of $1/\tau$ affects all Drude carriers, which highlights the transient excess scattering enabled by the presence of photoinduced quasiparticles.
[19] A. Lohner, M. Woerner, T. Elsaesser, and W. Kaiser, Phys. Rev. Lett. **68**, 3920 (1992).
[20] S. B. Kaplan *et al.*, Phys. Rev. **B14**, 4854 (1976).

[21] J.-J. Chang and D. J. Scalapino, Phys. Rev. **B15**, 2651 (1977).
[22] E. J. Nicol and J. P. Carbotte, Phys. Rev. **B67**, 214506 (2003).
[23] A. Rothwarf and B. N. Taylor, Phys. Rev. Lett. **19**, 27 (1967).
[24] D. Twerenbold, Phys. Rev. **B34**, 7748 (1986).
[25] G. L. Carr, R. P. S. M. Lobo, J. LaVeigne, D. H. Reitze, and D. B. Tanner, Phys. Rev. Lett. **85**, 3001 (2000).
[26] B. J. Feenstra *et al.*, Phys. Rev. Lett. **79**, 4890 (1997).
[27] T. Valla *et al.*, Science **285**, 2110 (1999).
[28] M. A. Quijada *et al.*, Phys Rev **B60**, 14917 (1999).